Where Does an Enzyme Reside in a Bicontinuous Structure?

Stefan Wellert[1,*], *Sandra* Engelskirchen[2], *Thomas* Hellweg[3], and *Olaf* Holderer[4,**]

[1]Department of Chemistry, Technische Universität Berlin, Berlin, Germany
[2]Department of Chemistry, Universität Stuttgart, Stuttgart, Germany
[3]Department of Chemistry, Physical and Biophysical Chemistry, Bielefeld University, Bielefeld, Germany
[4]Jülich Centre for Neutron Science (JCNS) at Heinz Maier-Leibnitz Zentrum (MLZ), Forschungszentrum Jülich GmbH, Garching, Germany

Abstract. Using enzymes as catalysts in biochemical processes requires to bring them into close contact with the substrates to be processed. For oil-soluble substrates and water soluble enzymes this might be achieved by bringing the water and oil phase in a bicontinuous microemulsion into close contact. In this contribution we review two possible scenarios of how the enzyme and the interface influence each other. Small angle neutron scattering (SANS) and neutron spin echo spectroscopy (NSE) act as a microscope to look into the details of the interfacial region of microemulsions.

1 Introduction

Microemulsions as thermodynamically stable mixtures of oil, water and surfactant, can provide a very unique environment for enzymatic catalysis. The thermodynamically stable compartmentalization of polar and non-polar phases by a large internal interface in the range of m^2/ml inspired the use of microemulsions as reaction media for a series of catalytic reactions, e.g. [1]. Among them, enzyme-catalyzed reactions are of particular interest. Domains of water and oil are only nanometers apart from each other, and provide therefore a very elegant way of bringing water soluble enzymes and often unpolar substrates together [2–4]. Depending on their macromolecular structure, the enzymes can accumulate either within the aqueous phase or directly at the amphiphilic interface. It can be assumed that an enzyme without enrichment at the interface has no influence on the mechanics, whereas an interfacially active enzyme should lead to changes in the mechanical properties in a concentration-dependent manner. Corresponding effects have already been observed with the addition of amphiphilic polymers (boosting).
Additives to microemulsions on the other hand can modify the location of phase boundaries in the phase diagram [5–7]. Mainly the elasticity of the surfactant layer separating oil and water is modified by incorporation of molecules [8] or co-surfactants [9, 10]. Neutron small angle scattering (SANS) and neutron spin echo spectroscopy (NSE) are scattering techniques which can provide a valuable insight into these systems structured on nanometer length scales, by combining structural information from SANS [11] and dynamic information about fluctuations from NSE [7, 12]. The influence of enzymes has been investigated with SANS and NSE for two different systems [13, 14]. This contribution reviews briefly how additives modify microemulsions, and how scattering techniques can scrutinize their enzyme induced changes in nanoscale structure and motion. The focus is thereby on the addition of proteins as bio-catalysts to microemulsion. Besides different interactions between enzymes and surfactant layers of the microemulsion, also the domain size of the microemulsion itself influences the physical properties of the system. The question of the relevance of density fluctuations or breathing modes in microemulsions will be addressed.

2 Microemulsions and Enzymes

Two main aspects of enzyme containing microemulsions will be briefly reviewed. On the one hand, the elastic properties of the surfactant membrane of microemulsions, described by the bending rigidity κ and saddle splay modulus $\bar{\kappa}$ relate the structure of the microemulsion to its dynamics. The addition of enzymes to the water phase of the emulsion might influence both, structure and dynamics depending how and where the enzymes reside. This is illustrated in figure showing in sketch a) the different possible locations and in b) an SEM measurement of the bicontinuous structure. [13].

2.1 Microemulsions as Compartments and Reaction Media

Microemulsions form two types of compartments, droplets (oil-in-water or water-in-oil) and bicontiuous structures. Here we focus only on the bicontiuous case. In bicontinuous microemulsions the two immiscible liquids (such as oil and water) are stabilized by a surfactant and are dispersed into each other, forming continuously connected but separated networks of both phases. The key advan-

*e-mail: s.wellert@tu-berlin.de
**e-mail: o.holderer@fz-juelich.de

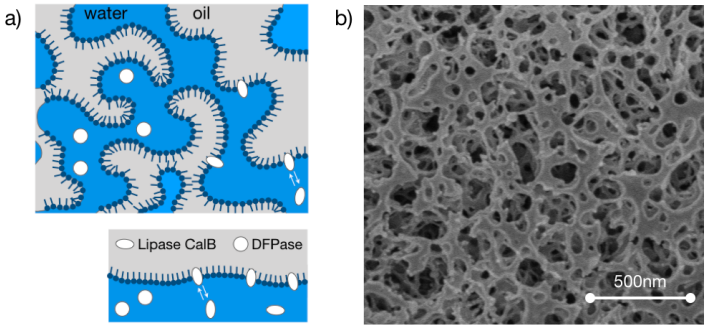

Figure 1. a) Top: Scenarios of enzyme – membrane interactions in microemulsions. Enzymes can be purely dissolved in water, rather unaffected by the presence of the lipid or surfactant interface, or they can interact and adsorb (for some residence time) at the interface. Bottom: When residing at the interface the presence of the enzyme can influence the bending elasticity of the interface and therefore the thermally activated fluctuations.
b) Freeze fracture SEM micrograph of a bicontinuous microemulsion structure which serves as the host medium in the discussed experiments.

tage is their enormous interfacial area, which facilitates mass transfer across the interface enhancing reaction constants of the reaction kinetics. Additionally, the bicontinuous structure also provides a highly stable environment for the reactants, potentially preventing unwanted side reactions or product degradation, since products and reactants are mainly separated via the interface. For example, the activity of DFPase remained high also in the complex environment of a mircoemulsion [13].

Bicontinuous microemulsions have been successfully employed in a wide range of chemical reactions, including organic synthesis, enzymatic reactions, and catalysis[15–17]. The potential of bicontinuous microemulsions in various fields such as pharmaceuticals, materials science, and biotechnology makes them a promising area of research for future applications.

2.2 Bicontinuous Microemulsions

As mentioned before, the bicontinuous structure resembles a sponge. The structural parameters, that is the domain size D_{TS} and the correlation length ξ_{TS} are obtained from fit of SANS measurements with the well-known Teubner-Strey formula [11]:

$$I_{\mathrm{TS}}(Q) = \frac{8\pi\langle\nu^2\rangle/\xi_{TS}}{p^2 - 2Q_{\mathrm{max}}^2 Q^2 + Q^4} \tag{1}$$

with $p^2 = (2\pi/D_{\mathrm{TS}})^2 + 1/\xi_{\mathrm{TS}}^2$ and $Q_{\mathrm{max}}^2 = (2\pi/D_{\mathrm{TS}})^2 - 1/\xi_{\mathrm{TS}}^2$. These measurements are performed in "bulk contrast", where D_2O and hydrogenated oil provide different scattering length densities for the two main domains in the sample.

2.3 Bicontinuous Microemulsion Membrane Dynamics

The Helfrich free energy is typically the starting point for considerations about the membrane structure and dynamics [18]. It reads

$$F_{el} = \int dS\,[\frac{\kappa}{2}(c_1 + c_2 - 2c_0)^2 + \bar{\kappa}c_1c_2] \tag{2}$$

where the principal curvatures c_1 and c_2, the mean curvature c_0 and the bending rigidities κ and $\bar{\kappa}$ are related.

Here, the bending rigidity κ determines the energy required to deviate the interfacial film from the spontaneous curvature c_0 at the given minimum of the free energy. The saddle-splay modulus $\bar{\kappa}$ gives the energy cost for saddle-splay deformations [19]. The bending elasticity constant is highly sensitive to any changes in topology and interfacial composition. And it is directly accessible by scattering in an easy way. A softening of the interfacial film is observed when undulations are thermally activated in the order of k_BT. This leads to a length scale dependent modification of the bare bending rigidity κ_0, the so-called renormalized bending elasticity constant:

$$\frac{\kappa_{\mathrm{SANS}}}{k_{\mathrm{B}}T} = \frac{\kappa_{0,\mathrm{SANS}}}{k_{\mathrm{B}}T} - \frac{3}{4\pi}\ln\left(\frac{D_{\mathrm{TS}}}{2l_{\mathrm{s}}}\right) \tag{3}$$

where the renormalization term contains the menbrane thickness l_s and therefore $D_{\mathrm{TS}}/2l_s$ is the membrane volume fraction.

This quantity is connected to the structural length scales inside the bicontinuous structure by [20]:

$$\frac{\kappa_{\mathrm{SANS}}}{k_{\mathrm{B}}T} = \frac{10\pi\sqrt{3}}{64}\frac{\xi_{\mathrm{TS}}}{D_{\mathrm{TS}}} \tag{4}$$

Simulations [21] in combination with measurements of the phase behavior, SANS and NSE experiments [22] revealed that the bending rigidity obtained with SANS are a combination of κ and $\bar{\kappa}$, $\kappa_{0,SANS} = (a_1\kappa_0 + a_2|\bar{\kappa}_0|)$. Also the renormalization term in Equation 3 is modified and reads $(3a_1 + 10/3|a_2|)/(4\pi)\ln(D_{TS}/2l_s)$ with $a_1 = 0.19$ and $a_2 = -0.84$ [22]. These corrections have been applied for the values of the bending rigidity from SANS measurements discussed here.
While the main structural features are obtained by fits with the Teubner-Strey structure factor [5, 11] as described above, the height fluctuations of the interface layer, governed by the film elasticity, are obtained in the framework of the Zilman-Granek model [12] from NSE mea-

surements. The contrast applied here is typically "film contrast", with only the interface layer made up from hydrogenated components, water and oil are deuterated (although at higher scattering vectors also "bulk contrast" samples provide the interface fluctuations in NSE). For relatively stiff membranes the intermediate scattering function from NSE can be approximated by a stretched exponential function, for softer membranes some modifications are required, e.g. by numerical integration of the correlation function [7]. But also the approach with the stretched exponential function results in the correct length scale dependence (i.e. the relaxation rate $\Gamma \propto q^3$) and the right curve shape of S(q,t) with a stretching exponent of $\beta = 2/3$. NSE experiments provide therefore the bending rigidity determined from height fluctuations in a rather direct way, while also SANS provides elastic properties from the ratio of the involved length scales of domain size and correlation length, which includes length scale dependent renormalization effects and also includes contributions from the saddle splay modulus [21, 22].

3 Experimental Aspects

3.1 The Microemulsion Systems

The results discussed in this contribution were obatined from scattering experiments with two microemulsion systems. A bicontinuous microemulsion from the ternary system pentaethylene glycol monodecyl ether($C_{10}E_5$)-D_2O/NaCl(4 wt.%)-d(18)-octane was used. Details of the phase behavior of the pure system and the system with additional lipase calB can be found in the literature [14].
The amphiphilic component of the second microemulsion system consists of a sugar surfactant ($C_{8/10}G_{1.3}$) and a medium chain alcohol (pentanol). In this case, instead of the temperature the alcohol content is used to tune the curvature of the amphiphilic film and to control the phase behavior. The quaternary system cyclohexane-D_2O-$C_{8/10}G_{1.3}$-pentanol resembles all structural features of a ternary system using the pentanol content as tuning parameter.[13]
All samples were prepared near the X-point of the respective phase diagram. The position of the phase boundaries for each sample was visually determined prior to the measurements. All bicontinuous samples used in the experiments were prepared at an oil-to-water ratio α=0.5. The surfactant concentration γ in case of the ternary system was γ=0.15 irrespective of the enzyme concentration. The temperature was 35.5° C for the blank microemulsion going down to 24.5° C when the enzyme concentration was raised up to 100mg/ml. In case of the quaternary system, the surfactant concentration was at γ=0.21 with a concentration δ=0.06 of pentanol serving as cosurfactant in the amphiphilic component.

3.2 The Enzymes lipase CalB and DFPase

Lipases show the technically interesting tendency to adsorb to oil-water interfaces which leads to a restructuring of the enzyme at the interface and in fact activates the enzyme (at least the wild type).
The enzyme diisopropyl fluorophosphatase (DFPase) from the squid Loligo vulgaris belongs to a group of enzymes that efficiently detoxify highly toxic organophosphorus (OP) compounds, which act as irreversible inhibitors of acetylcholinesterase [23]. DFPase has a remarkable thermal stability and is very tolerant toward organic solvents which makes it an excellent candidate for an catalytic additive inside a microemulsion. Moreover, DFPase can routinely be produced by heterologous expression in E. coli. The lipase from Candida antarctica B (CalB) is from a broad class of enzymes which have the potential of acting as catalyzers for organic reactions with often only poorly water soluble substrates, which makes such microemulsion systems with the proximity of water and oil phases a very attractive environment.
Experimental details related to the expression, purification and characterization of the enzymes and their introduction with different concentration into the buffered aqueous phases of the microemulsions were previously described in the literature [13, 14].
The enzyme concentrations used vary widely and were mainly chosen with regard to the technically desirable quantities in each case.

Protein	conc. (mg/ml)	Surfactant	Oil phase
CalB	0	$C_{10}E_5$	octane
CalB	10	$C_{10}E_5$	octane
CalB	50	$C_{10}E_5$	octane
CalB	100	$C_{10}E_5$	octane
DFPase	0	$C_{8/10}G_{1.3}$/pent.	cyclohexane
DFPase	5	$C_{8/10}G_{1.3}$/pent.	cyclohexane
DFPase	10	$C_{8/10}G_{1.3}$/pent.	cyclohexane

Table 1. Sample composition of the investigated microemulsions.

3.3 Measurement of Membrane Fluctuations

Neutron spin echo spectroscopy (NSE) uses spin encoding and decoding of the neutron spin velocity by a large number of spin precessions in a magnetic field before and after the scattering in the sample [24]. This decouples the energy resolution from the wavelength spread $d\lambda/\lambda$ of the neutron beam and allows to use a relatively broad wavelength band (typically 10-20 %) by providing a very high energy resolution. The actually measured signal is the Fourier transform of the scattering function from the energy domain to the time domain, the intermediate scattering function S(Q,τ_{NSE}). A high energy resolution is equivalent to a large Fourier time obtained at the NSE. For a Lorentzian line broadening with a FWHM Γ in energy space, the Fourier transform leads to an exponential decay with relaxation time τ [ns] = 1.317 / Γ[μeV] (see e.g. [25]). The intermediate scattering function is the time correlation function in reciprocal space, in the case of bicontinuous microemulsion this reflects the height fluctuations of the surfactant membrane on the relevant NSE length scales.

The NSE bending rigidity is obtained from the full integration of the Zilman-Granek model [7, 12]:

$$S(Q,\tau_{\mathrm{NSE}}) \propto \int_0^1 d\mu \int_0^R dr\, rJ_0\left(Qr\sqrt{1-\mu^2}\right) \exp\left(-\frac{k_{\mathrm{B}}T}{2\pi\kappa}Q^2\mu^2\int_{k_{\min}}^{k_{\max}}\frac{dk}{k^3}\left(1-J_0(kr)e^{-\omega(k)t}\right)\right) \quad (5)$$

with the Bessel function $J_0(kr)$ and the integration limits of the membrane undulations, k_{min} and k_{max}, which correspond to the maximum and minimum undulation wavelength respectively present in the microemulsion membrane.

4 Results

4.1 On the Analysis of Intermediate Scattering Functions in the Case of a Bicontinuous Microemulsion

Two main dynamical processes may occur in the time and length scale window of typical NSE experiments. On larger length scales, density fluctuations or "breathing modes" might be present, which show a typical Q^2 dependence of the relaxation rate similar to simple diffusion. On shorter length scales, the Q^3 behaviour and the stretched exponential decay of the Zilman-Granek model dominates [22, 26]. Density fluctuations may well be observed with dynamic light scattering [9]. Their contribution can be included into the data modelling by an additional diffusive Q^2-dependent decay, a path which has been followed in Ref. [13]. If one assumes, both modes of motion to be decoupled from each other, the result is an additive superposition of their contributions. However, if the breathing motion and interfacial fluctuations depend on each other in the time and size range accessible with a NSE measurement, their contributions must be considered accordingly.

$$S(Q,\tau_{NSE})/S(Q,0) = exp(-\Gamma_{col}\tau_{NSE})(A + (1-A)\, exp(-(\Gamma_u\tau_{NSE})^{\beta}) \quad (6)$$

The two relaxation rates here are the collective relaxation rate Γ_{col}, which is related to a diffusive Q^2 dependent decay, and the undulation relaxation rate of a membrane patch, Γ_u. Plotting the resulting values of Γ_u vs. Q^3 yields the bending elastic constant κ_{NSE} according to

$$\Gamma_u = 0.025\gamma_\kappa\left(\frac{k_BT}{\kappa_{NSE}}\right)^{1/2}\frac{k_BT}{\eta_{eff}}Q^3 \quad (7)$$

Here, η_{eff} is the effective solvent viscosity of the fluid surrounding the fluctuating membranes and γ_κ is a numerical parameter.

Taking a look at the microemulsions used there and fitting the dynamics for a series of scattering vectors simultaneously either purely with the full Zilman-Granek model with numerical integration from Ref [7], or with the additional diffusive contribution. Figure 2 shows the data with this simultaneous fits. Only including the diffusion allows to reproduce the decay of the intermediate scattering functions correctly, the diffusion constant D_{col}=Γ_{col}/Q^2 with

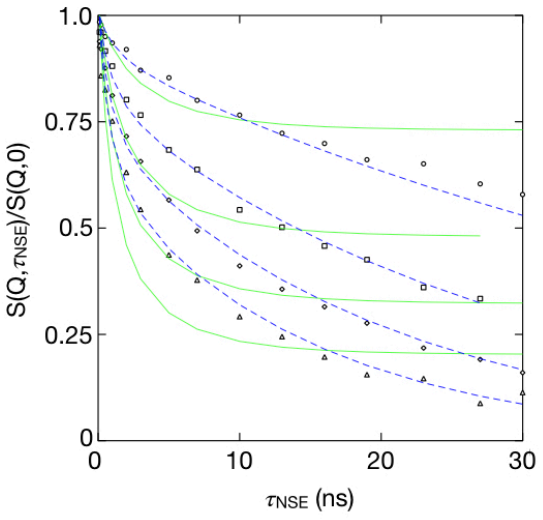

Figure 2. Normalized intermediate scattering functions of a pure film contrast microemulsion, used for the measurements on the microemulsions dynamics in case of addition of DFPase in Ref. [13]. The blue symbols mark the data points for a set of four Q values (0.05 Å^{-1} to 0.24 Å^{-1}), the dashed line shows the fits to the data points calculated with the fully dynamic structure factor including a diffusive mode while the solid lines in green show the result where only the undulation mode is visible in the time and length scale window of NSE (Γ_{col} = 0 in Eq. 6)

.

this simultaneous fit is $1.49 \pm 0.02 \times 10^{-1}$ cm^2/s, very similar to the 1.75×10^{-1} cm^2/s reported in Ref. [13] from DLS measurements. The form of Eq. 6 allows for multiplicative diffusive motion (which is visible on top of the membrane undulations, i.e. the undulations follow additionally the density fluctuations), or decoupled to some extend (by the factor A).

The microemulsions used with CalB in Ref. [14] had a significantly larger domain size than the sugar surfactant based microemulsion shown in Fig. 2. The reason for the difference is most probably the different domain size and hence different length scale where density fluctuations play a role. A smaller domain size shifts the region where density fluctuations are relevant into the window accessible by NSE. Length scale (or q-)dependent evaluation is then required and possible, and the diffusive contribution can be deduced, either directly from NSE experiments (provided the data quality and q-t-range is sufficient), or by an additional DLS measurement.

An interesting theoretical problem remains in the prediction at which domain sizes the signature of the breathing modes has to be included into the analysis. Up to now, only the actual analysis process can answer this question for the respective investigated system.

4.2 On the Effect of the Enzymes on the Membrane Fluctuation Dynamics

Two experiments will be compared here: the microemulsion structure and dynamics of the protein DFPase in a sugar surfactant based microemulsion, as reported in [13],

and the enzyme CalB in a nonionic surfactant based microemulsion [14].

From the protein point of view, there is one major difference which is worth a direct comparison. The bending elasticity measured with NSE and SANS should both depend in the same way on the protein concentration.

Figure 3 compiles the bending rigidities determined with NSE and SANS for the two systems from Refs. [13] and [14]. The observed κ values are within the observation window constant with protein concentration for the DFPase, but not equal between NSE and SANS. For CalB, the NSE bending rigidity slight increases, while the one determined from the structure via SANS slightly decreases. The slight decrease from the structural determination is interpreted similar to the effect of adding homopolymers to a bicontinuous microemulsion [27] ("anti-boosting effect"). It is obtained from SANS, which measures a snapshot of the fluctuating structure, which is then averaged over many "snapshots" during the time of the measurement. NSE on the other hand provides insight into the local shape fluctuations on nanosecond time scales and provides therefore a different view on the elasticity. Adsorption may result in a stiffening of the membrane visible in the increase in κ from NSE. This behaviour might reflect the temporary adsorption of the lipase at the interface and a kinetic exchange equilibrium with the lipase residing in the aqueous phase. This is in contrast to the DFPase mainly dissolved in the water phase. The bending rigidities of the DFPase containing microemulsion differs significantly between NSE and SANS. The pure $\kappa_{0,NSE}$ shows this behaviour with the full integration of the Zilman-Granek model (which takes into account the undulation spectrum of the membrane) as well as the stretched exponential simplified model (which might take a too broad undulation spectrum, often corrected for with an adapted viscosity of the surrounding medium). The reason for the difference might be the rather medium efficient technical grade sugar surfactant, which requires a high surfactant concentration and a locally very croweded environment. The additional distance to the X-point in the phase diagram might change the contribution of κ and $\bar{\kappa}$ to the SANS bending rigidity, or in a simple picture the time averaged structure seems to be rather disordered compared to the high energy needed to bend the membrane. The role of the average viscosity which affects the diffusive as well as the undulation modes in the microemulsion is more complex in such technical grade high concentration microemulsions and need further attention. A more detailed view into this question requires additional experiments.

5 Conclusion

Two bicontinuous microemulsion systems with enzymes introduced in the aqueous phase are revisited and compared. The structure and dynamics measured with SANS and NSE provide interesting insights and details about the effect of the enzyme on the elastic properties of the surfactant membrane of the microemulsion. The enzyme can either be mainly dissolved in the water phase with no significant influence on the membrane elasticity as in the case of DFPase which lacks an amphiphilic character, or it can

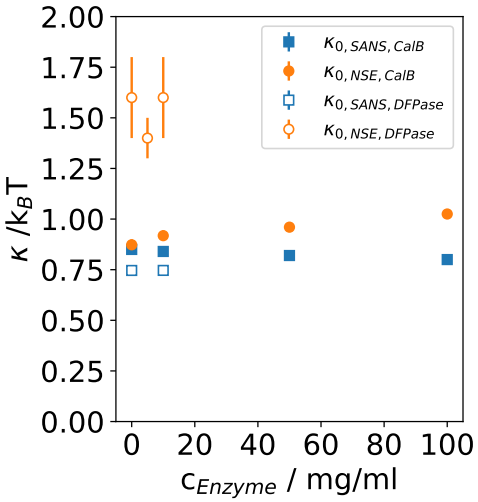

Figure 3. Comparison of bending rigidities from DFPase and CalB determined from structural data (SANS) and from membrane height fluctuations (NSE). Data are from Refs. [14] and [13].

modify the bending elasticity as in the case of CalB which can undergo conformational changes at a water-oil interface, where NSE reveals on nanosecond time scales a stiffening of the amphiphilic membrane, while SANS with its time averaged measurement shows the opposite effect. It has been suggested that the residence time of the protein CalB at the surfactant interface is the origin of this result. The reason why the DFPase does not change κ significantly, for example similar to the reduction in κ observed upon homopolymer addition into microemulsion phases as in Ref. [6], is a bit speculative. It may be that having the not surface active component only in the water phase is not sufficient for affecting the conformational space of the membrane and thus reducing κ. However, since also a combined effect of κ and $\bar{\kappa}$ could lead to this results, future measurements on both bending elasticity constants in droplet microemulsions could provide additional insights.

A second observation between the two systems under investigation is the relevance of breathing modes observable in the membrane dynamics depending on the characteristic size of the domains of the microemulsion. With smaller structures, the importance of breathing modes observed on the length scales accessible with NSE increases. The coupling of breathing modes with the undulation modes might be also a topic of further study.

Further experiments might shed light on the interfacial activity of enzymes in microemulsions and on the influence of the structural length scales of the microemulsion on its dynamics as well as on possible enzymatic activities. Such experiments can in future support theoretical considerations to predict the potential interfacial activity of enzymes.

Acknowledgement

This work is based upon experiments performed at the J-NSE instrument operated by Forschungszentrum Jülich at the Heinz Maier-Leibnitz Zentrum (MLZ), Garching, Germany.

References

[1] B. Orlich, R. Schomäcker, Enzyme Microb. Technol. **28**, 42 (2001)

[2] M. Subinya, A.K. Steudle, B. Nestl, B. Nebel, B. Hauer, C. Stubenrauch, S. Engelskirchen, Langmuir **30**, 2993 (2014)

[3] K. Homberg, Adv. Colloid Interf. Sci. **51**, 137 (1994)

[4] S. Serrano-Luginbühl, K. Ruiz-Mirazo, R. Ostaszewski, F. Gallo, P. Walde, Nature Rev. Chem. **2**, 306 (2018)

[5] C. Frank, H. Frielinghaus, J. Allgaier, H. Prast, Langmuir **23**, 6526 (2007)

[6] O. Holderer, H. Frielinghaus, D. Byelov, M. Monkenbusch, J. Allgaier, D. Richter, Journal of Chemical Physics **122** (2005)

[7] M. Mihailescu, M. Monkenbusch, H. Endo, J. Allgaier, G. Gompper, J. Stellbrink, D. Richter, B. Jakobs, T. Sottmann, B. Farago, The Journal of Chemical Physics **115**, 9563 (2001)

[8] H. Klemmer, H. Frielinghaus, J. Allgaier, M. Ohl, O. Holderer (2017), Vol. 862, ISSN 17426596

[9] S. Wellert, H.J. Altmann, A. Richardt, A. Lapp, P. Falus, B. Farago, T. Hellweg, The European Physical Journal E **33**, 243 (2010)

[10] H. Klemmer, J. Allgaier, H. Frielinghaus, O. Holderer, M. Ohl, Colloid and Polymer Science **295** (2017)

[11] M. Teubner, R. Strey, The Journal of Chemical Physics **87**, 3195 (1987)

[12] A.G. Zilman, R. Granek, Physical review letters **77**, 4788 (1996)

[13] S. Wellert, B. Tiersch, J. Koetz, A. Richardt, A. Lapp, O. Holderer, J. Gäb, M.M. Blum, C. Schulreich, R. Stehle et al., European Biophysics Journal **40** (2011)

[14] S. Engelskirchen, S. Wellert, O. Holderer, H. Frielinghaus, M. Laupheimer, S. Richter, B. Nestl, B. Nebel, B. Hauer, Frontiers in Chemistry **8**, 613388 (2021)

[15] M.J. Schwager, K. Stickdorn, R. Schomäcker, Chem. Rev. **95**, 849 (1995)

[16] K. Homberg, Eur. J. Org. Chem. **2007**, 731 (2007)

[17] K.M. Larsson, P. Adlercreutz, B. Mattlasson, J. Chem. Soc. Faraday Trans. **87**, 465 (1991)

[18] W. Helfrich, Zeitschrift für Naturforschung A **33**, 305 (1978)

[19] S. Safran, Advances in physics **48**, 395 (1999)

[20] P. Pieruschka, S. Safran, S. Marcelja, Physical Review E **52**, 1245 (1995)

[21] M. Peltomäki, G. Gompper, D.M. Kroll, The Journal of chemical physics **136**, 134708 (2012)

[22] O. Holderer, H. Frielinghaus, M. Monkenbusch, M. Klostermann, T. Sottmann, D. Richter, Soft Matter **9** (2013)

[23] M. Blum, F. Löhr, A. Richardt, H. Rüterjans, J.C.H. Chen, J. Am. Chem. Soc. **128**, 1275012757 (2006)

[24] F. Mezei, ed., *Neutron Spin Echo*, Vol. 128 (Springer Berlin Heidelberg, 1980), ISBN 978-3-540-10004-1

[25] F. Mezei, C. Pappas, T. Gutberlet, eds., *Neutron Spin Echo Spectroscopy*, Vol. 601 (Springer Berlin Heidelberg, 2003), ISBN 978-3-540-44293-6

[26] M. Monkenbusch, O. Holderer, H. Frielinghaus, D. Byelov, J. Allgaier, D. Richter, Journal of Physics Condensed Matter **17** (2005)

[27] D. Byelov, H. Frielinghaus, O. Holderer, J. Allgaier, D. Richter, Langmuir **20** (2004)